

Sequential Neural Rendering with Transformer

Phong Ha Nguyen¹, Lam Huynh¹, Esa Rahtu², and Janne Heikkilä¹

¹ Center for Machine Vision and Signal Analysis, University of Oulu, Finland

² Tampere University, Finland
phong.nguyen@oulu.fi

Abstract. This paper address the problem of novel view synthesis by means of neural rendering, where we are interested in predicting the novel view at an arbitrary camera pose based on a given set of input images from other viewpoints. Using the known query pose and input poses, we create an ordered set of observations that leads to the target view. Thus, the problem of single novel view synthesis is reformulated as a sequential view prediction task. In this paper, the proposed Transformer-based Generative Query Network (T-GQN) extends the neural-rendering methods by adding two new concepts. First, we use multi-view attention learning between context images to obtain multiple implicit scene representations. Second, we introduce a sequential rendering decoder to predict an image sequence, including the target view, based on the learned representations. We evaluate our model on various challenging synthetic datasets and demonstrate that our model can give consistent predictions and achieve faster training convergence than the former architectures.

Keywords: multi-view attention, novel view synthesis, transformers

1 Introduction

View synthesis aims to creating novel views of an object or a scene from a perspective of a virtual camera based on a set of reference images. It has been an active field of research already for several decades in computer vision and computer graphics due to its various application areas including free-viewpoint television, virtual and augmented reality, and telepresence [2,35,32,16,20].

Conventionally, the view synthesis problem has been addressed by using image-based or geometry-based approaches [2]. In pure image-based rendering, the novel view is warped from a densely sampled set of reference images or the light field without exploiting any geometric information, which obviously requires a large amount of image data and limits the new viewpoints to a relatively small range. In geometry-based rendering, the novel view is generated using a 3D model that has been first created from the reference views using multi-view stereo or some other image-based modeling techniques. This allows for larger baselines between the views, but also sets high requirements to the quality of the 3D model. Between these two extremes, free viewpoint depth-image-based rendering (DIBR) uses depth maps associated to the reference views enabling

3D image warping to synthesize the novel view [32]. In practice, all these approaches tend to produce notable artifacts due to missing or inaccurate data, which reduced the quality of the rendered image.

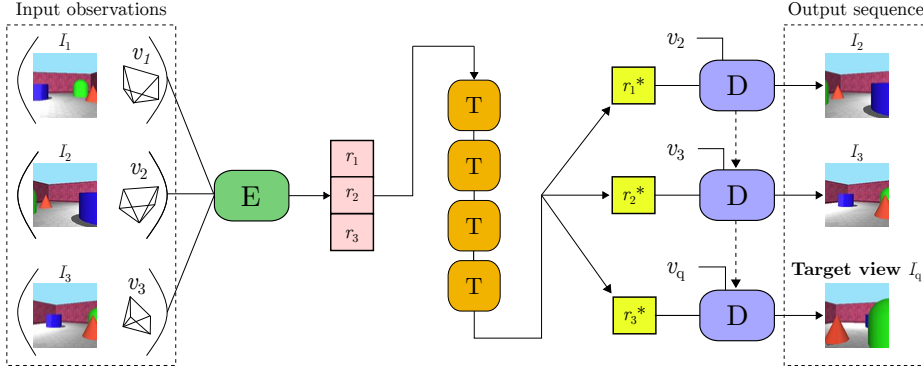


Fig. 1. Overview of our proposed Transformer-based Generative Query Network (T-GQN). Given a set of input images and camera poses $\{(I_n, v_n)\}$, where $n = 1, \dots, N$, we obtain a set of N scene representations by passing them one-by-one through the encoder (E) network. We use a stack of transformer encoder (T) to perform the multi-view attention learning between these representation. Finally, we use each these attention representation r_n^* to sequentially render the output sequence using the decoder (D) network. The dashed arrow indicates that we initialize states of the decoder network with the computed states of the previous step.

Recently, researchers have adopted deep learning techniques to overcome the inherent limitation of the conventional approaches. This paper focused on a family of neural rendering methods [7,29,21,23,37] that have shown promising result by introducing a generative model that understands the underlying 3D scene structure and faithfully produces the target view even at a distant query pose. These methods use an aggregate function to represent the entire 3D scene as a single implicit representation. Although they manage to successfully render the target view, they are required to be trained on a large amount of data, which in turn, takes a long time to reach the convergence. We argue that because these methods focus on synthesizing only a single target image, they are inefficient when rendering target images for distant query poses that are subject to strong geometric transformations and occlusions with respect to the reference images.

In this paper, we introduce a Transformer-based Generative Query Network (T-GQN) to address the problem of novel view synthesis in a sequential manner. We train an end-to-end model that sequentially renders a positionally ordered set of nearby-views and then predicts the target view at the final rendering step (as shown in Fig. 1). We claim that if the model is able to render the nearby-views accurately, it will be also capable of predicting the target view correctly. Since we do not have the nearby-views of the target pose, we train our model to

render the input views. Moreover, instead of rendering the viewpoints using a single implicit scene representation, we use multi-view attention learning based on Transformer Encoder [38] to learn multiple scene representations. At each rendering step, we modify the decoder network of Generative Query Network (GQN) [7] to share its states through rendering steps. To summarize, our key contributions are as follows:

1. We reformulate the problem of single view synthesis into sequential view synthesis.
2. Our proposed T-GQN introduces two novel concepts: multi-view attention learning via the Transformer Encoder and a sequential rendering decoder. Our model extends the previously proposed GQN by sequentially rendering a pose-ordered set of novel views.
3. We demonstrate that our proposed framework achieves state-of-the-art performance on challenging view synthesis datasets. Moreover, our method reaches convergence faster and requires less computational resource to train.

The source code and the model will be made publicly available upon publication of the paper.

2 Related Work

The literature related to view synthesis is extensive, and to limit the scope, we focus on a few deep learning based methods in this section that are most relevant to our method.

Image-to-image translation refers to transforming an image from one domain to another. The task of novel view synthesis can be also considered as an image-to-image translation problem where the target and the source domains are defined by the camera poses. While most of the research in the field focuses only on texture transfer, changing the viewpoint requires more complicated domain specification and understanding of the 3D geometry. In recent years, Generative Adversarial Networks (GANs)[12] have become the most popular approach for image-to-image-translation, and they have been also successfully used for novel view synthesis. For example, [25] proposes a method for generation of new views of a scene given a single input image, and in [9], authors show that they can perform iterative object manipulation to steer the transformation using the adversarial training. However, their work is limited to a single rotated object while our work shows a strong generalization to novel viewpoints and objects.

A great amount of effort has been dedicated to incorporate geometric information to the model. For example, [8,40,17,33,4] apply deep learning techniques to leverage geometry cues and learn to predict the novel view. The deep learning based-light field camera view interpolation [17,22] use a deep network to predict depth separately for every novel view. Another line of work [8,40,33] cleverly extract a layered representation of the scene. The layers, which they learn to

combine into the novel view, offer a regularization that allows for an impressive stereo base-line extrapolation. Recently, Choi et al.[4] use deep neural network to estimate a depth probability volume, rather than just a single depth value for each pixel of the novel view. Even though, they show promising results but they are limited to synthesizing a middle view among source images or a magnified view from a single input. In contrast, our proposed framework focuses on arbitrary target views and is able to learn from source images vary in length.

Many early solutions use regression to derive the pixel colors of the target view directly from the input images. In [36], Tatarchenko et al. maps an image of a scene to an RGB-D image from an unknown viewpoint with an auto-encoder architecture and train their model using supervised learning. Instead of synthesizing pixels from scratch, other works explores using CNNs to predict appearance flow [41]. Later work by Sun et al. [34] presents a self-confidence aggregation mechanism to integrate both predicted appearance flow and pixel hallucination to achieve contractually consistent results.

Another line of work [26,3,24] use 3D convolution layers to learn 3D spatial transformations from the input views to the novel view and then apply GAN training [12] to enhance quality of the output image. However, their results are limited to a scene with a single object [39] or a slight change in viewpoints in the autonomous driving situation [11]. Recently, Sitzman et al.[31] presents a continuous, 3D-structure-aware scene representation that encodes both geometry and appearance. Their works learns a mapping from world coordinates to feature representation of local scene properties. However, their deterministic architecture does not generalized well in novel scenes which are not a part of the training set. By contrast, we are interested in synthesizing novel views in probabilistic-manner so that the network can learn to deal with general objects and scenes.

Recent **neural rendering** methods have introduced a generative model that understands the underlying 3D scene structure and faithfully produces the target view at the distant query pose. However, Generative Query Network (GQN) [7] and its variant [29,21,23] are incorporating all input observation (images and poses) into a single implicit 3D scene representation to generate the target view. This aggregated representation contains all necessary information (e.g. object identities, positions, colors, scene layout) to make accurate image predictions. In this paper, we argue that generating the target view using such compact representation leads to poor predictions and slow training convergence.

In [37], authors introduce GQN with Epipolar Cross-Attention (E-GQN), which leverage the geometric relationship between camera viewpoints to learn the epipolar representation of the scenes. Then, they apply attention mechanism to have multiple scene representation at each rendering step. The drawback of their method is that it requires extra memory to store those epipolar representations for each input observation. By contrast, our proposed multi-view attention representations are being shared across the rendering step. Therefore, our proposed framework is lighter and requires less memory to train than the former architecture.

3 Approach

In this section, we first provide the reader with a brief background of Generative Query Network (GQN). Then we convert the problem of **single view synthesis** to the problem of **sequential view synthesis** by introducing our Transformer-based Generative Query Network (T-GQN) that extends the current GQN architecture with two novel building blocks: multi-view attention learning via Transformer Encoder and sequential rendering decoder.

3.1 Generative Query Network

Given the observations that include N images $I_n \in I$ and their corresponding camera poses $v_n \in V$, GQN [7] solves the **single view synthesis** problem by using a encoder-decoder neural network to predict the target image I_q at an arbitrary query pose v_q .

First, the encoder is a feed-forward neural network that take N observations as input and produce a single implicit scene representation $R = \sum_{n=1}^N r_n$ by performing a element-wise sum of N encoded scene representation r_n . The decoder then takes R and v_q as an input and predicts the new view I'_q from that viewpoint. The decoder network is a conditional latent variable model DRAW [14,13] which includes M pairs of Generation and Inference convolutional LSTM networks. At each generation step, the hidden state of the Generation and Inference LSTM core is utilized to approximate the prior π and posterior distribution q . Since the target view I_q is fed into the Inference sub-network, minimizing the Kullback-Leibler (KL) distance between π and q would help the Generation sub-network to produce the accurate result. Both the encoder and decoder network are trained jointly to minimize the ELBO loss \mathcal{L}_{GQN} function:

$$\mathcal{L}_{GQN} = \left[-\ln \mathcal{N}(I_q|I'_q) + \sum_{m=1}^M KL[\mathcal{N}(q_m)||\mathcal{N}(\pi_m)] \right] \quad (1)$$

Later, in the experimental results, we show that training GQN using the above \mathcal{L}_{GQN} loss takes a long time to reach the convergence (as shown in Fig. 8). In the next section, we will describe how we reformulate the problem of **single view synthesis** to the problem of **sequential view synthesis** to address this issue.

3.2 Sequential view synthesis

As can be seen from Fig. 2 (a), GQN [7] predicts the target view I_q in a single rendering step. If the query pose v_q is distant with all input poses then the target view might be completely different from all input views. In this case, minimizing the above \mathcal{L}_{GQN} loss does not guarantee to generate a plausible target view and it might take a long training time to reach the convergence.

We argue that if the model is able to predict an input view I'_n for $n > 1$ based on previous input data $\{(I_1, v_1), \dots, (I_{n-1}, v_{n-1})\}$ then it has better capability of

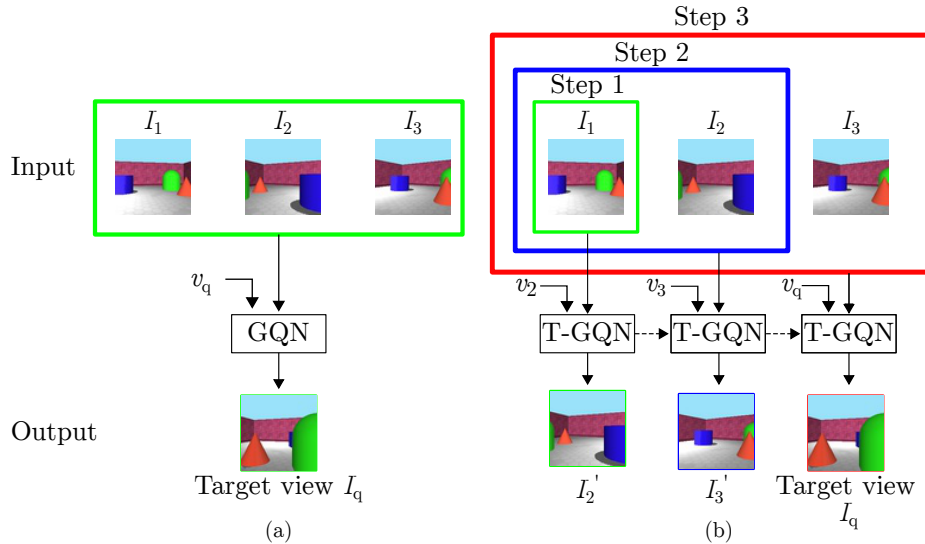


Fig. 2. An illustration of the single view synthesis (a) compared to our proposed sequential view synthesis (b). Previously proposed GQN [7] directly predicts the target view in a single rendering step, while our proposed T-GQN sequentially predicts novel views from an ordered set of N observations. The output set includes $N - 1$ nearest views of the target view and the target view itself. Colored boxes indicate which input observations are encoded at each rendering step. Note that we can freely choose which input observations to be encoded via the attention mask of the Transformer Encoder.

rendering also the target view I_q at the query pose v_q provided that the camera poses $\{v_1, \dots, v_N, v_q\}$ have been organized as a sequence where the adjacent poses are the closest ones. To achieve such ability, we train our proposed T-GQN model using multiple rendering steps. Each rendering step of our model is identical with GQN except that we use different sets of input observations and query poses. In Fig. 2 (b) we illustrate these sets of input observations at each rendering step with boxes of different colors.

For example, in the first rendering step, we only allow the model to use the information inside the green box which includes the input view I_1 and its camera pose v_1 . Then, our T-GQN model is trained to predict the next input view I_2' at the viewpoint v_2 . Preventing the model to look at the input view I_2 would encourage the model to learn to extrapolate viewpoints beyond the given information. In the final rendering step, both GQN and our proposed T-GQN model are allowed to see all N input observations to render the target view but our model can leverage the past experiences from previous rendering steps to have a better approximation I_q' of the target image I_q . Furthermore, training our model in multiple rendering steps enforces our model to make consistent predictions of novel views at different viewpoints in a forwards pass. This helps to stabilize

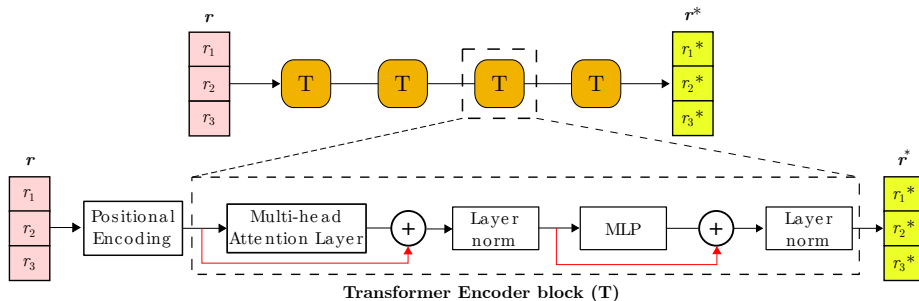


Fig. 3. Illustration of multi-view attention learning using a stack of Transformer Encoder (T) blocks. For the visualization purposes, we show how a single Transformer Encoder block is able to produce multiple implicit scene representations r^* using the input view representations r .

the training process by making the network to produce deterministic results and also be able to reach the convergence faster than the former architecture.

Therefore, the problem of single view synthesis can be redefined as the problem of sequential view synthesis by predicting a sequence of N novel views $S_{out} = \{I'_2, \dots, I'_N, I'_q\}$ from a sequence of observations $S_{in} = \{(I_1, v_1), \dots, (I_N, v_N)\}$. Since we are having N different target views then it would be beneficial to have N different scene representations. In order to have such multiple implicit scene representations, we use the Transformer Encoder [38] to learn the dependencies between input observations at each rendering step.

3.3 Multi-view attention learning via Transformer Encoder

Recent works in the Language Modeling task [38,6,28,5] use the self attention-based Transformer Encoder to effectively learn dependencies between word embeddings in a sentence. Transformer Encoder takes a set of word embeddings as an input and produces another set of enhanced word embedding representations. Each of these representations reflects the long-range dependencies between input embeddings and they have been proven to be useful for training various language modeling tasks. Therefore, we can also take a set of scene representations r as an input and use the Transformer Encoder to produce another set of enhanced scene representations r^* that are trained to exploit the multi-view dependencies.

Fig. 3 shows an example of how we use a stack of Transformer Encoder blocks to perform the multi-view attention learning and implicitly represent a scene using a set of multiple representations. Within a Transformer Encoder block, the most important component is the Multi-Head Attention layer using the self-attention mechanism [38]. The self-attention function produces an $N \times N$ matrix A of multi-view attention scores so that each row of the matrix A reflects the learned multi-view dependencies at each rendering step. In addition, we apply an attention mask m to the multi-view attention scores A . This attention mask allows us to control which part of the input representation sequence r we would

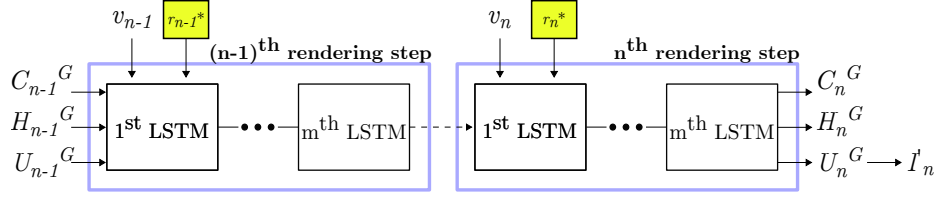


Fig. 4. Illustration of our proposed sequential rendering decoder. At each rendering step, we use the computed states from the previous rendering step as the initialization for the decoder network. The canvas state U_n^G is utilized to render the novel image I'_n .

like the model to ignore when computing the attention scores. In practice, we found that applying this attention mask leads to better performance on datasets that have high similarities between viewpoints. When the input viewpoints are not overlapping, we found that better results are achieved without applying the attention mask. We will discuss more about this attention mask and its usage in Section 5. Moreover, we leave the implementation details of Transformer Encoder in the supplementary material.

3.4 Sequential rendering decoder

In this paper, we improve the decoder network of GQN [7] by applying a recurrent mechanism between rendering steps. In order to transfer the knowledge between rendering steps, computed LSTM states from previous steps are utilized as initialization for the current step as shown in the Fig. 4. Here, we simplify the notation by defining that C_n^G is the cell state of the m^{th} Generation core at the n^{th} rendering step. We apply this kind of notation to all cell states C , hidden states H and canvas states U of the decoder network. At the n^{th} rendering step, the novel image I'_n is computed as follows:

$$I'_n = \text{decoder}(r_n^*, v_n, C_{n-1}^G, H_{n-1}^G, U_{n-1}^G, C_{n-1}^I, H_{n-1}^I) \quad (2)$$

Since our model has multiple rendering steps, the prior and the posterior terms, π_n^m and q_n^m , are obtained from the m^{th} LSTM core at the n^{th} rendering step. We train our model using the modified ELBO loss function as follows:

$$\mathcal{L}_{TGQN} = \left[- \sum_{n=1}^N \ln \mathcal{N}(I_n | I'_n) + \beta \sum_{n=1}^N \sum_{m=1}^M \text{KL}[\mathcal{N}(q_n^m) || \mathcal{N}(\pi_n^m)] \right] \quad (3)$$

By adding the β coefficient to the KL term, we emphasize discovering the disentangled latent factors [19]. This technique has proven to be effective to maximize the probability of generating the desired output and keeping the distance between the prior and posterior distribution small [15].

4 Experiments

4.1 Datasets

We compare the performance of our proposed T-GQN with GQN [7] and E-GQN [37]. We use two datasets, Rooms-Ring-Camera (RRC) and Rooms-Free-Camera (RFC), from [7] and one dataset, Rooms-Random-Objects (RRO), from [37].

The RRC dataset contains various rendered 3D square rooms that are composed of random objects of various shapes, colors and locations. Moreover, the scene textures, walls and lights are also randomly generated. In this dataset, the camera only moves on a fixed ring and always faces the center of the room. In case of the RFC dataset, the environment is the same with RRC except for the freely moving camera and objects rotated around their vertical axes. We also evaluate our method on the RRO dataset which includes complex 3D scenes with realistic 3D objects from the ShapeNet dataset [1].

4.2 Experimental setup

To create a sequence of adjacent poses, we could, for example, use the overlap between the viewing frustums of the cameras to measure their adjacency. However, in our experiments we simply reordered all input observations based on the Euclidean distance between the translation vector of the query pose and the input poses that turned out to be sufficient to demonstrate the efficiency of our method. We choose to train our T-GQN model using three input observations to render a target view at an arbitrary query pose. We adopt the Pool Encoder network from [7] so that each encoded scene representation r_n is a vector of 256 values. As can be seen from Fig. 3, we add a positional encoding vector to each of the encoded scene representation before feeding them to the Transformer Encoder. Instead of using the learned positional vector [10], we choose the fixated version from [38]. To learn the multi-view attention representation, we use a stack of four Transformer Encoders. In each of the Transformer Encoder, the MLP block contains two linear layers. The dimensionality of the input and the output of this MLP block is 256, and the second linear layer has the dimensionality of 512. We also apply a residual dropout with a rate of 0.1 for each of the residual connection (red line in the Fig. 3).

Our decoder network architecture is adopted from [7] (see Figure S2) with the exception of our extended recurrent mechanism between multiple rendering steps. All cell states, hidden states and canvas states of a LSTM core have 128 channels in case of training RRC and RFC datasets. In case of training the RRO dataset, we increase the number of channel to 256 due to a broader range of complex objects in the dataset. The original GQN architecture consumes a large amount of computing and memory resources. Due to computational restrictions, we demonstrate the advantages of the proposed architectural changes using less LSTM cores than in [7]. Originally, training a 12 layer-LSTM GQN model with batch size of 36 requires four NVIDIA K80 GPUs as described in [7]. In this

Table 1. Quantitative comparison of results between our T-GQN model, original GQN [7] and E-GQN [37].

Model	# parameters (millions)	L1 (pixels)			L2 (pixels)			SSIM		
		RRC	RFC	RRO	RRC	RFC	RRO	RRC	RFC	RRO
GQN(8 LSTM layers)	381	8.5	14.23	14.12	18.62	30.28	21.79	0.81	0.75	0.74
GQN(12 LSTM layers)	428	7.40	12.44	10.12	14.62	26.80	19.63	0.85	0.79	0.81
E-GQN	N/A	3.59	12.05	6.59	6.80	27.65	12.08	N/A	N/A	N/A
T-GQN without attention mask	382	3.30	4.25	6.31	6.65	5.75	11.72	0.91	0.89	0.82
T-GQN with attention mask	382	2.31	11.65	5.28	5.92	15.44	11.65	0.92	0.82	0.85

paper, we use a single Tesla P100 GPU to train our T-GQN model which has only eight LSTM layers and our training batch size is 24.

We implement our models on PyTorch [27] and train them using ADAM optimizer [18] with hyper-parameter: $\beta_1 = 0.9$ and $\beta_2 = 0.999$. We train our model over one million iterations with the same annealing learning rate as in [7]. Instead of using the same annealing pixel-variance strategy as in [7], we keep the pixel-variance at 2.0 for the first 100k iterations, at 0.2 for the next 100k iterations followed by 0.4 for the next 100k iterations, and then finally leave it at 1.0 until the end of the training. The intuition is to keep the pixel-variance high first so that the model can learn to create the general structure of the novel view first. After that we reduce the pixel-variance so that the model can focus more on rendering small details later. We did some hyper-parameter sweep tests and found that keeping the pixel-variance at 1.0 gives a good balance between prior and posterior distributions.

4.3 Results

We use L_1 , L_2 and structural similarity measure (SSIM) to assess the quality of the predicted novel image with respect to ground-truth target image on the held-out test set. Table 1 and Fig. 5 show the quantitative and some qualitative results of all methods after training. Overall, our method outperforms the baselines on all three datasets.

As can be seen from Table 1, training our T-GQN model with the attention mask leads to a performance gain on the RRC and RRO datasets. In the case of the RFC dataset, our method without the attention mask leads to a bigger performance gap compared to other methods including ours with the attention mask. Qualitative results shown in Fig. 5 demonstrate that the T-GQN model with or without the attention mask is able to render all novel images much sharper than the former architectures. Meanwhile, predicted target views from GQN [7] are often blurry and not able to get the correct object types, colors and positions.

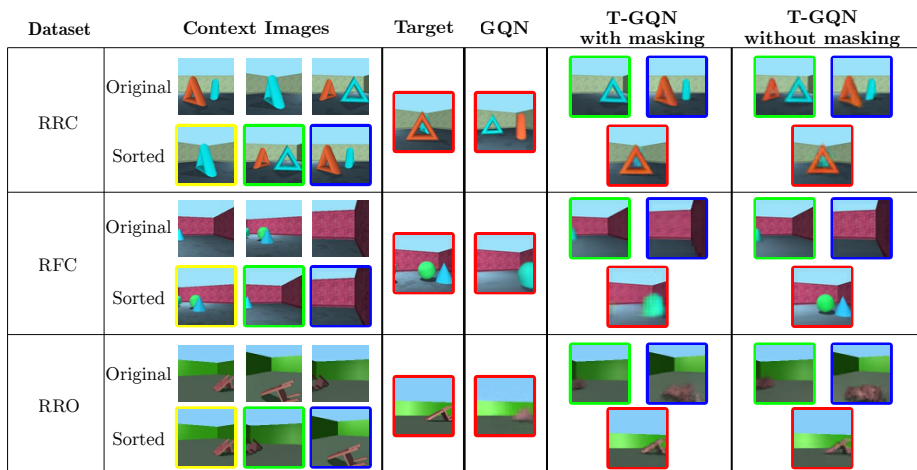







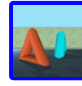



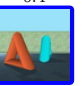


Fig. 5. Example of rendered novel views using our proposed T-GQN (with and without masking) and other methods. We manually put colored boxes to easily compare the rendering quality between the ground-truth and predicted novel views. Overall, our proposed T-GQN model is able to produce better target view than previous methods. More examples can be found in the Appendix section.

Our T-GQN model also has an advantage in the number of parameters over the former architectures. Using the same amount of LSTM layers in the decoder, our T-GQN model clearly outperforms the baseline GQN by adding only extra one million trainable parameters of Transformer Encoder. In addition, our method needs only a single GPU for training, but manages to produce significantly better results than the recently proposed E-GQN, which has more trainable parameters and requires 4-8 Tesla-V100 to train [37].










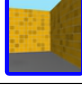





5 Discussion

Experimental results on the RRC and RRO datasets show that our T-GQN model with the attention mask is able to produce better results when the movement of the camera is restricted. In the RFC dataset, the camera is allowed to move freely and applying the attention mask to our model leads to performance degradation. In this section, we analyze the experimental results by visualizing the multi-view attention scores (as described in Section 3.3) at each rendering step for each case. Visualizing these scores would help to understand how our proposed model is able to render the novel views.

If the movement of the camera is restricted then input viewpoints are overlapped with each other. Therefore, masking the attention scores would mean that the model is trained to predict the novel view using only a subset of the input sequence. Fig. 6 (a) shows the multi-view attention scores of a camera-restricted example from RRC dataset. In the 1st rendering step, we try to render the 2nd

Rendering step	Input			Ground-truth	Predicted
1	1.0 				
2	0.24 	0.76 			
3	0.15 	0.45 	0.4 		

(a)

Rendering step	Input			Ground-truth	Predicted
1	0.05 	0.92 	0.03 		
2	0.04 	0.1 	0.86 		
3	0.01 	0.95 	0.04 		

(b)

Fig. 6. Visualization of multi-view attention scores at each rendering step produced by our methods when (a) the camera movement is restricted and (b) the camera is free to move.

input view (green box) as the novel view. Since our model is only allowed to use the 1st view (yellow box) as the input, the predicted image only contains the cyan object. However, our model is able to render the missing orange object by putting higher scores on the 2nd input view in the next rendering step. Since the 1st input view does not have enough information to render the target view, our model learns to give it less attention and produce higher attention scores on another two input views.

In the RFC dataset, the camera movement is not restricted so that the input sequence might contain views which do not include necessary information to render the target view. In this case, we allow the model to use all input observations by not applying the attention mask. In Fig. 6 (b), our model is able to give high attention scores to input observations which are the ground-truth views in the first two rendering steps. Therefore, the first two predicted novel views are iden-

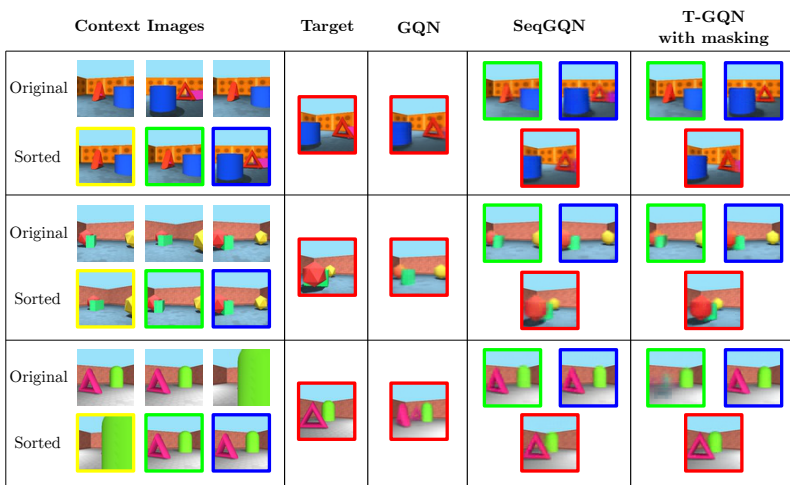


Fig. 7. Example of generated novel views compared between our proposed T-GQN and variants on the RRC dataset.

Table 2. Quantitative results of T-GQN and its variants on the Rooms-Ring-Camera dataset.

Metric	GQN	SeqGQN	T-GQN ($\beta = 1$)	T-GQN ($\beta = 250$)
L1 (pixels)	7.40	4.51	3.7	2.31
L2 (pixels)	14.62	8.2	7.1	5.92
SSIM	0.85	0.882	0.905	0.92

tical to the ground-truth because the model has already seen these novel views as inputs. However, our goal is to be able to predict the target view (red box) which has a distant query pose. Among three input observations, the 2nd input is the only view which contains information about objects on the scene. As can be seen in the last rendering steps, our model manages to pay most attention on the 2nd input view (green box) and gives low scores to the other two views and successfully predicts the target view despite the distant query pose.

6 Ablation Study

To investigate the effectiveness of the proposed modules, we use our sequential rendering decoder to generate novel views using the aggregated scene representation R from [7] and denote this model as SeqGQN. Instead of using different multi-view attention representations at each rendering step, we use a single representation R as an input to all LSTM layers in our proposed sequential rendering decoder network. The qualitative and quantitative results including the rendered novel views using SeqGQN can be found from Fig. 7 and Table 2. We observe

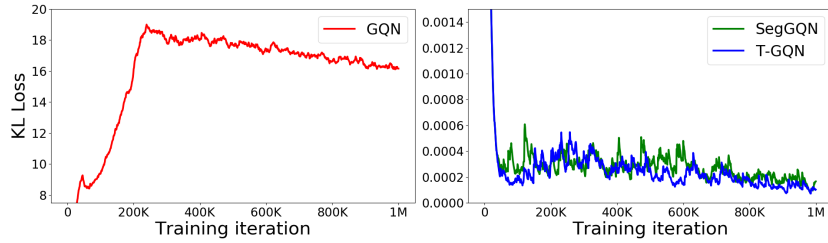


Fig. 8. Comparison of the KL loss between GQN, SeqGQN and our T-GQN. Both SeqGQN and T-GQN are using the sequential rendering decoder with $\beta = 250$.

Table 3. Comparison of quantitative results between our T-GQN models using a different number of Transformer Encoders to learn the multi-view dependencies. Note that we only apply the attention mask in training our T-GQN model with the RRC and the RRO datasets. In case of the RFC dataset, we do not use the attention mask.

Model	L1 (pixels)			L2 (pixels)			SSIM		
	RRC	RFC	RRO	RRC	RFC	RRO	RRC	RFC	RRO
T-GQN (1 Transformer Encoder)	3.45	5.7	6.27	6.87	8.59	13.85	0.87	0.85	0.81
T-GQN (4 Transformer Encoders)	2.31	4.25	5.28	5.92	5.75	11.65	0.92	0.89	0.85
T-GQN (8 Transformer Encoders)	2.32	4.25	5.31	5.93	5.75	11.7	0.92	0.89	0.84

that our full model significantly outperforms both SeqGQN and GQN. Although both GQN and SeqGQN are using the same aggregated scene representation R , SeqGQN is able to produce better and more accurate target views than the baseline. This result demonstrates that approaching the neural rendering in the sequential manner leads to more accurate view synthesis.

Since we are adding a large β coefficient into the KL loss term (Eq. 3), we are encouraging the model to approximate the posterior distribution q_n^m close to the prior distribution π_n^m as much as possible. If the query pose is far away from given input observations then it is hard to get a good estimate for q_n^m . In [7], the model is prone to mistakes because the target view is rendered in a single step. Using the sequential rendering decoder, we solve the problem by generating the near-by views of the target view before rendering the target view. As can be seen from Table 2, training our T-GQN model with $\beta = 1$ leads to a drop of the overall performance. However, this model is still able to outperform both GQN and SeqGQN. Fig. 8 shows the KL loss during the training procedure of GQN, SeqGQN and T-GQN. At the end of the training, the KL loss of GQN is higher than both SeqGQN and T-GQN with quite a large margin. This indicates that our model is able to reach convergence faster than the former architecture.

Moreover, we investigate on the effect of Transformer Encoders to our proposed method. Table 3 shows the quantitative results of training T-GQN using different numbers of Transformer Encoders. We can see that training the T-GQN model using a block of 4 Transformer Encoders leads to a slight increase in performance compared to just using a single Transformer Encoder block. In contrast, increasing the number of Transformer Encoder to 8 does not improve the overall performance as shown in the Table 3. Thus, we suggest using a stack of 4 Transformer Encoders to effectively learn the multi-view dependencies without using a larger model.

7 Conclusions

In this paper, we presented a method to synthesize novel views in a sequential manner. Instead of directly rendering the target view, we train our model to predict a sequence of novel views in multiple rendering steps. Using the Transformer Encoder, our proposed multi-view attention learning is able to learn different implicit scene representations for each rendering step. The experimental results demonstrate that our model is able to render more accurate novel views and reach convergence faster than former architectures. In our future work, we will explore how to generate novel views of indoor scenes in a bigger scale including more objects and different lightning conditions.

References

1. Chang, A.X., Funkhouser, T., Guibas, L., Hanrahan, P., Huang, Q., Li, Z., Savarese, S., Savva, M., Song, S., Su, H., Xiao, J., Yi, L., Yu, F.: Shapenet: An information-rich 3d model repository (2015)
2. CHANG, Y., WANG, G.P.: A review on image-based rendering. *Virtual Reality & Intelligent Hardware* **1**(1), 39 – 54 (2019). <https://doi.org/https://doi.org/10.3724/SP.J.2096-5796.2018.0004>, <http://www.sciencedirect.com/science/article/pii/S2096579619300051>
3. Chen, X., Song, J., Hilliges, O.: Monocular neural image based rendering with continuous view control. In: *Proceedings of the IEEE International Conference on Computer Vision*. pp. 4090–4100 (2019)
4. Choi, I., Gallo, O., Troccoli, A., Kim, M.H., Kautz, J.: Extreme view synthesis. In: *Proceedings of the IEEE International Conference on Computer Vision*. pp. 7781–7790 (2019)
5. Dai, Z., Yang, Z., Yang, Y., Carbonell, J., Le, Q., Salakhutdinov, R.: Transformer-XL: Attentive language models beyond a fixed-length context. In: *Proceedings of the 57th Annual Meeting of the Association for Computational Linguistics*. pp. 2978–2988. Association for Computational Linguistics, Florence, Italy (Jul 2019). <https://doi.org/10.18653/v1/P19-1285>, <https://www.aclweb.org/anthology/P19-1285>
6. Devlin, J., Chang, M.W., Lee, K., Toutanova, K.: BERT: Pre-training of deep bidirectional transformers for language understanding. In: *Proceedings of the 2019 Conference of the North American Chapter of the Association for Computational Linguistics: Human Language Technologies, Volume 1 (Long and Short*

- Papers). pp. 4171–4186. Association for Computational Linguistics, Minneapolis, Minnesota (Jun 2019). <https://doi.org/10.18653/v1/N19-1423>, <https://www.aclweb.org/anthology/N19-1423>
7. Eslami, S.A., Rezende, D.J., Besse, F., Viola, F., Morcos, A.S., Garnelo, M., Ruder-
man, A., Rusu, A.A., Danihelka, I., Gregor, K., et al.: Neural scene representation
and rendering. *Science* **360**(6394), 1204–1210 (2018)
 8. Flynn, J., Neulander, I., Philbin, J., Snavely, N.: Deep stereo: Learning to pre-
dict new views from the world’s imagery. In: 2016 IEEE Conference on Com-
puter Vision and Pattern Recognition (CVPR). pp. 5515–5524 (June 2016).
<https://doi.org/10.1109/CVPR.2016.595>
 9. Galama, Y., Mensink, T.: Itergans: Iterative gans to learn and control 3d object
transformation. *Computer Vision and Image Understanding* **189**, 102803 (2019)
 10. Gehring, J., Auli, M., Grangier, D., Yarats, D., Dauphin, Y.N.: Convolutional
sequence to sequence learning. In: Precup, D., Teh, Y.W. (eds.) Proceedings of
the 34th International Conference on Machine Learning. Proceedings of Machine
Learning Research, vol. 70, pp. 1243–1252. PMLR, International Convention Cen-
tre, Sydney, Australia (06–11 Aug 2017), [http://proceedings.mlr.press/v70/
gehring17a.html](http://proceedings.mlr.press/v70/gehring17a.html)
 11. Geiger, A., Lenz, P., Urtasun, R.: Are we ready for autonomous driv-
ing? the kitti vision benchmark suite. In: 2012 IEEE Conference on
Computer Vision and Pattern Recognition. pp. 3354–3361 (June 2012).
<https://doi.org/10.1109/CVPR.2012.6248074>
 12. Goodfellow, I., Pouget-Abadie, J., Mirza, M., Xu, B., Warde-Farley, D., Ozair, S.,
Courville, A., Bengio, Y.: Generative adversarial nets. In: Ghahramani, Z., Welling,
M., Cortes, C., Lawrence, N.D., Weinberger, K.Q. (eds.) Advances in Neural In-
formation Processing Systems 27, pp. 2672–2680. Curran Associates, Inc. (2014),
<http://papers.nips.cc/paper/5423-generative-adversarial-nets.pdf>
 13. Gregor, K., Besse, F., Jimenez Rezende, D., Danihelka, I., Wierstra, D.: Towards
conceptual compression. In: Lee, D.D., Sugiyama, M., Luxburg, U.V., Guyon,
I., Garnett, R. (eds.) Advances in Neural Information Processing Systems 29,
pp. 3549–3557. Curran Associates, Inc. (2016), [http://papers.nips.cc/paper/
6542-towards-conceptual-compression.pdf](http://papers.nips.cc/paper/6542-towards-conceptual-compression.pdf)
 14. Gregor, K., Danihelka, I., Graves, A., Rezende, D., Wierstra, D.: Draw: A recurrent
neural network for image generation. In: Bach, F., Blei, D. (eds.) Proceedings of
the 32nd International Conference on Machine Learning. Proceedings of Machine
Learning Research, vol. 37, pp. 1462–1471. PMLR, Lille, France (07–09 Jul 2015),
<http://proceedings.mlr.press/v37/gregor15.html>
 15. Higgins, I., Matthey, L., Pal, A., Burgess, C., Glorot, X., Botvinick, M.M., Mo-
hamed, S., Lerchner, A.: beta-vae: Learning basic visual concepts with a con-
strained variational framework. In: ICLR (2017)
 16. Joachimczak, M., Liu, J., Ando, H.: Real-time mixed-reality telepresence
via 3d reconstruction with hololens and commodity depth sensors. In: Pro-
ceedings of the 19th ACM International Conference on Multimodal Interac-
tion. p. 514515. ICMI 17, Association for Computing Machinery, New York,
NY, USA (2017). <https://doi.org/10.1145/3136755.3143031>, [https://doi.org/
10.1145/3136755.3143031](https://doi.org/10.1145/3136755.3143031)
 17. Kalantari, N.K., Wang, T.C., Ramamoorthi, R.: Learning-based view syn-
thesis for light field cameras. *ACM Trans. Graph.* **35**(6) (Nov 2016).
<https://doi.org/10.1145/2980179.2980251>, [https://doi.org/10.1145/2980179.
2980251](https://doi.org/10.1145/2980179.2980251)

18. Kingma, D.P., Ba, J.: Adam: A method for stochastic optimization (2014)
19. Kingma, D.P., Welling, M.: An introduction to variational autoencoders. *Foundations and Trends in Machine Learning* **12**(4), 307–392 (2019). <https://doi.org/10.1561/22000000056>, <https://doi.org/10.1561/22000000056>
20. Kolkmeier, J., Harmsen, E., Giesselink, S., Reidsma, D., Theune, M., Heylen, D.: With a little help from a holographic friend: The openimpress mixed reality telepresence toolkit for remote collaboration systems. In: *Proceedings of the 24th ACM Symposium on Virtual Reality Software and Technology. VRST 18*, Association for Computing Machinery, New York, NY, USA (2018). <https://doi.org/10.1145/3281505.3281542>, <https://doi.org/10.1145/3281505.3281542>
21. Kumar, A., Eslami, S., Rezende, D.J., Garnelo, M., Viola, F., Lockhart, E., Shananhan, M.: Consistent generative query networks. *arXiv preprint arXiv:1807.02033* (2018)
22. Mildenhall, B., Srinivasan, P.P., Ortiz-Cayon, R., Kalantari, N.K., Ramamoorthi, R., Ng, R., Kar, A.: Local light field fusion: Practical view synthesis with prescriptive sampling guidelines. *ACM Trans. Graph.* **38**(4) (Jul 2019). <https://doi.org/10.1145/3306346.3322980>, <https://doi.org/10.1145/3306346.3322980>
23. Nguyen-Ha, P., Huynh, L., Rahtu, E., Heikkilä, J.: Predicting novel views using generative adversarial query network. In: *Scandinavian Conference on Image Analysis*. pp. 16–27. Springer (2019)
24. Nguyen-Phuoc, T., Li, C., Theis, L., Richardt, C., Yang, Y.L.: Hologan: Unsupervised learning of 3d representations from natural images. In: *The IEEE International Conference on Computer Vision (ICCV)* (Nov 2019)
25. Olivia Wiles, Georgia Gkioxari, R.S.J.J.: SynSin: End-to-end view synthesis from a single image. *CVPR* (2020)
26. Olszewski, K., Tulyakov, S., Woodford, O., Li, H., Luo, L.: Transformable bottleneck networks. *The IEEE International Conference on Computer Vision (ICCV)* (Nov 2019)
27. Paszke, A., Gross, S., Massa, F., Lerer, A., Bradbury, J., Chanan, G., Killeen, T., Lin, Z., Gimelshein, N., Antiga, L., Desmaison, A., Kopf, A., Yang, E., DeVito, Z., Raison, M., Tejani, A., Chilamkurthy, S., Steiner, B., Fang, L., Bai, J., Chintala, S.: Pytorch: An imperative style, high-performance deep learning library. In: *Advances in Neural Information Processing Systems 32*, pp. 8026–8037. Curran Associates, Inc. (2019), <http://papers.nips.cc/paper/9015-pytorch-an-imperative-style-high-performance-deep-learning-library.pdf>
28. Radford, A., Wu, J., Child, R., Luan, D., Amodei, D., Sutskever, I.: Language models are unsupervised multitask learners. *OpenAI Blog* **1**(8), 9 (2019)
29. Rosenbaum, D., Besse, F., Viola, F., Rezende, D.J., Eslami, S.: Learning models for visual 3d localization with implicit mapping. *arXiv preprint arXiv:1807.03149* (2018)
30. Shi, X., Chen, Z., Wang, H., Yeung, D.Y., Wong, W.k., Woo, W.c.: Convolutional lstm network: A machine learning approach for precipitation nowcasting. In: *Proceedings of the 28th International Conference on Neural Information Processing Systems - Volume 1*. p. 802810. NIPS15, MIT Press, Cambridge, MA, USA (2015)
31. Sitzmann, V., Zollhoefer, M., Wetzstein, G.: Scene representation networks: Continuous 3d-structure-aware neural scene representations. In: *Advances in Neural Information Processing Systems 32*, pp. 1121–1132. Curran Associates, Inc. (2019), <http://papers.nips.cc/paper/>

- 8396-scene-representation-networks-continuous-3d-structure-aware-neural-scene-representations.pdf
32. Smirnov, S., Battisti, F., Gotchev, A.P.: Layered approach for improving the quality of free-viewpoint depth-image-based rendering images. *Journal of Electronic Imaging* **28**(1), 1 – 17 (2019). <https://doi.org/10.1117/1.JEI.28.1.013049>, <https://doi.org/10.1117/1.JEI.28.1.013049>
 33. Srinivasan, P.P., Tucker, R., Barron, J.T., Ramamoorthi, R., Ng, R., Snavely, N.: Pushing the boundaries of view extrapolation with multiplane images. In: *IEEE Conference on Computer Vision and Pattern Recognition, CVPR 2019, Long Beach, CA, USA, June 16-20, 2019*. pp. 175–184. Computer Vision Foundation / IEEE (2019). <https://doi.org/10.1109/CVPR.2019.00026>
 34. Sun, S.H., Huh, M., Liao, Y.H., Zhang, N., Lim, J.J.: Multi-view to novel view: Synthesizing novel views with self-learned confidence. In: *European Conference on Computer Vision (2018)*
 35. Tanimoto, M.: Ftv: Free-viewpoint television. *Signal Processing: Image Communication* **27**(6), 555 – 570 (2012). <https://doi.org/https://doi.org/10.1016/j.image.2012.02.016>, <http://www.sciencedirect.com/science/article/pii/S0923596512000495>
 36. Tatarchenko, M., Dosovitskiy, A., Brox, T.: Multi-view 3d models from single images with a convolutional network. In: *European Conference on Computer Vision (ECCV) (2016)*
 37. Tobin, J., Zaremba, W., Abbeel, P.: Geometry-aware neural rendering. In: *Advances in Neural Information Processing Systems 32*. Curran Associates, Inc. (2019), <http://papers.nips.cc/paper/9331-geometry-aware-neural-rendering.pdf>
 38. Vaswani, A., Shazeer, N., Parmar, N., Uszkoreit, J., Jones, L., Gomez, A.N., Kaiser, L.u., Polosukhin, I.: Attention is all you need. In: Guyon, I., Luxburg, U.V., Bengio, S., Wallach, H., Fergus, R., Vishwanathan, S., Garnett, R. (eds.) *Advances in Neural Information Processing Systems 30*, pp. 5998–6008. Curran Associates, Inc. (2017), <http://papers.nips.cc/paper/7181-attention-is-all-you-need.pdf>
 39. Zhirong Wu, Song, S., Khosla, A., Fisher Yu, Linguang Zhang, Xiaoou Tang, Xiao, J.: 3d shapenets: A deep representation for volumetric shapes. In: *2015 IEEE Conference on Computer Vision and Pattern Recognition (CVPR)*. pp. 1912–1920 (June 2015). <https://doi.org/10.1109/CVPR.2015.7298801>
 40. Zhou, T., Tucker, R., Flynn, J., Fyffe, G., Snavely, N.: Stereo magnification: Learning view synthesis using multiplane images. In: *SIGGRAPH (2018)*
 41. Zhou, T., Tulsiani, S., Sun, W., Malik, J., Efros, A.A.: View synthesis by appearance flow. *CoRR* **abs/1605.03557** (2016), <http://arxiv.org/abs/1605.03557>

Appendix of Sequential Neural Rendering with Transformer

The organization of the appendix is as follows. We present the network architecture details in section 1. In the section 1.2, we illustrate additional examples showing how our model produces multi-view attention scores to render the target view. In section 3, we present additional results of each rendering step using our proposed sequential neural rendering T-GQN model. Finally, we analyze the novel view rendering results qualitatively and quantitatively using different multi-view attention scene representations in section 4.

1 Details about the network architecture

1.1 Details about the encoder network

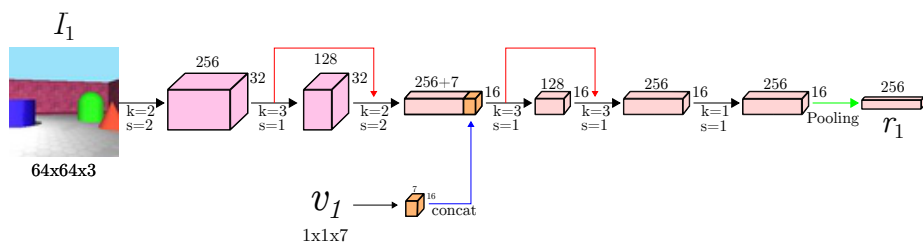


Fig. 9. The detailed architecture of the encoder network.

Fig. 9 shows how we use the encoder network to produce a scene representation r_n using an RGB image I_n and its camera pose v_n . In this paper, we adopt the Pool encoder architecture from GQN [7]. The input image has the spatial size of 64. All black arrows represent convolutional layers with kernel size k and stride s . Each convolutional layer is followed by an activation function. We choose to use Leaky ReLU instead of ReLU like [7]. The red arrows indicate the residual connections. The camera pose v_n is then broadcasted in the spatial dimensions to concatenate with the learned features after the first residual block. Finally, we perform average pooling (green arrow) with the size of 16 on the output of the last convolutional layer to obtain an encoded scene representation r_n as a vector of 256 values.

1.2 Details about the transformer encoder network

Fig. 10 illustrates the detailed architecture of a transformer encoder block. Within a Transformer Encoder block, the most important component is the Multi-Head Attention layer using the self-attention mechanism [38]. A key property of the self-attention model is that it has equivalent reordering, that is, it

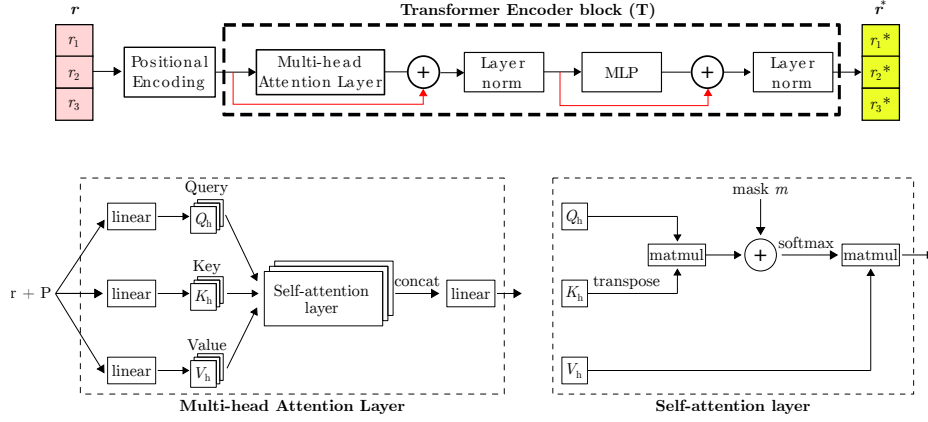


Fig. 10. The detailed architecture of the a transformer encoder block.

gives the same output independently of how N input representations are shuffled. This is problematic since we are sequentially rendering novel images in a specific order. To alleviate this limitation, we simply add a positional encoding P to the input representation r . Then we linearly project $(r + P)$ to different query Q , keys K , and value V representation. It has been found beneficial in [38] to replicate this self-attention mechanism into H heads, each being able to focus on different parts of the input by using different sets of query Q_h , key K_h and value V_h representations. Outputs from multiple heads are concatenated and then linearly projected to the original size of r using a projection weight W_{out} and a bias term b_{out} . The output of the Multi-head Attention Layer can be expressed as follows:

$$\text{Self-attention}_h(r + P) = \left[\text{softmax}(A_h + m) \right] V \quad (4)$$

$$m = \begin{pmatrix} 0 & -\infty & -\infty \\ 0 & 0 & -\infty \\ 0 & 0 & 0 \end{pmatrix} \text{ if } N = 3 \quad (5)$$

$$\text{Multi-head}(r + P) = \text{concat}_{h \in H} \left[\text{Self-Attention}_h(r + P) \right] W_{out} + b_{out} \quad (6)$$

where we refer to the elements of the $N \times N$ matrix $A_h = \frac{QK^\top}{\sqrt{s}}$ as attention values, the softmax output as attention probabilities and \sqrt{s} is the scaling factor.

1.3 Details about the sequential rendering decoder

Fig. 11 shows the detailed architecture of our proposed sequential rendering decoder. In this paper, we adopt the decoder network of GQN [7] and extend

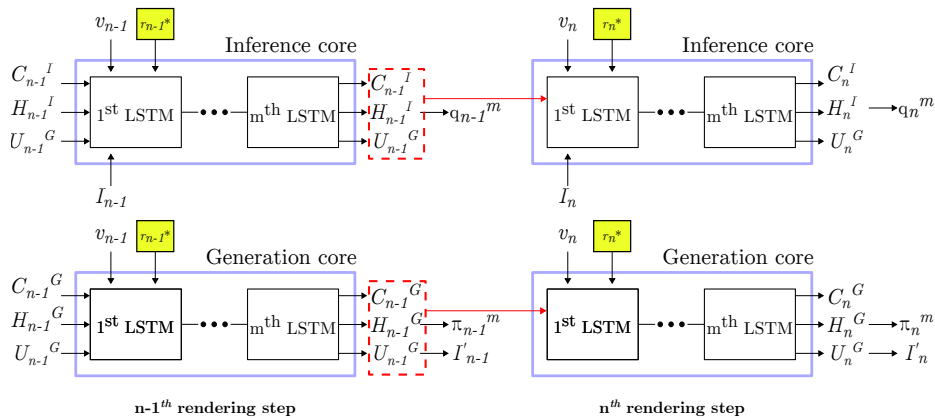


Fig. 11. The detailed architecture of the sequential rendering decoder. The red arrow indicates that all computed states of the Inference and Generation cores at the $n - 1^{th}$ are being transferred to the next rendering step.

it by perform neural rendering in multiple steps. The decoder network includes two different sub-networks: Inference core I and Generation core G . Both of them are based on the skip-connection Convolutional LSTM [30]. Each of these LSTM cores are parameterized by a cell state C , a hidden state H and a canvas state U . Using the hidden state H_n^I and H_n^G , we can approximate the posterior q_n^m and prior π_n^m normal distributions. Since the novel view I_n is fed into the Inference core I then minimizing the Kullback-Leibler (KL) distance between q_n^m and π_n^m would help the Generation core to produce the correct novel image I'_n in the testing phase.

In order to effectively transferring learned knowledge, all cell states, hidden states and canvas states of both Inference and Generation cores are being utilized as the initialization for all states of the next rendering step. In Fig. 11, states of the Inference and Generation cores at the $n - 1^{th}$ rendering steps are being transferred to the n^{th} rendering step.

2 Visualizing the multi-view attention scores

In this work, we employ $H = 8$ parallel self-attention layers in each block of Transformer Encoder so that each layer produces an instance of attention probabilities. Therefore, we take a mean operation over all these attention probabilities to produce a multi-view attention scores $S = \sum_{h=1}^H \text{softmax}(A_h + m)$. Fig. 12, 13 and 14 show examples of the multi-view attention scores on the held-out test set of the Rooms-Ring-Camera (RRC), Rooms-Free-Camera (RFC) and Rooms-Random-Objects (RRO) datasets, respectively.

Table 4. Quantitative comparison of results between our T-GQN models using the sequential rendering decoder (full model) and different multi-view attention scene representations (using r_1^*, r_2^*, r_3^*).

Model	L1 (pixels)			L2 (pixels)		
	RRC	RFC	RRO	RRC	RFC	RRO
T-GQN (using r_1^*)	3.28	5.42	6.19	7.26	6.97	13.68
T-GQN (using r_2^*)	2.35	4.37	5.58	6.98	6.46	13.25
T-GQN (using r_3^*)	2.30	4.32	5.34	6.03	5.98	12.04
T-GQN (full model)	2.31	4.25	5.28	5.92	5.75	11.65

3 Additional qualitative results

In this section, we provide additional qualitative results. Fig. 15, 16 and 17 show more examples of rendered novel views using our proposed T-GQN model and its variant GQN [7] on Rooms-Ring-Camera (RRC), Rooms-Free-Camera (RFC) and Rooms-Random-Objects (RRO) datasets, respectively.

4 A study about multi-view attention representations

In this paper, the full model of T-GQN uses a sequential rendering decoder to render the target novel view and we train our model using multiple rendering steps. At the n^{th} rendering step, a different multi-view attention scene representation r_n^* is fed into the decoder network to render the novel view I'_n at the viewpoint v_n . However, all of these scene representation r_n^* are outputs of the Transformer Encoder which already processes N input observations. Thus, each of these scene representation r_n^* is able to produce the target novel view I_q at the query pose v_q .

To investigate the effectiveness of all these learned scene representation r_n^* compared to our full model, we employ each of them as the input to the decoder network and predict the target image I_q at the query pose v_q in a single rendering step. We denoted these model as T-GQN(using r_n^*) and our proposed method is T-GQN (full model). Table 4 and Fig. 18 show the qualitative and quantitative results between our T-GQN (full model) and its variant T-GQN (using r_n^*). We observe that our full model of T-GQN is able to outperform other models across datasets. However, the T-GQN model using the scene representation r_3^* is on-par with the full model. This proves that the learned scene representation r_3^* is fully capable of rendering the target image I_q at the query pose v_q using just a single rendering step. Therefore, we only need to use the sequential rendering decoder in the training time. In the testing time, we can achieve almost the same rendered views using the scene representation r_3^* in a single rendering step as can be seen in Fig. 18.

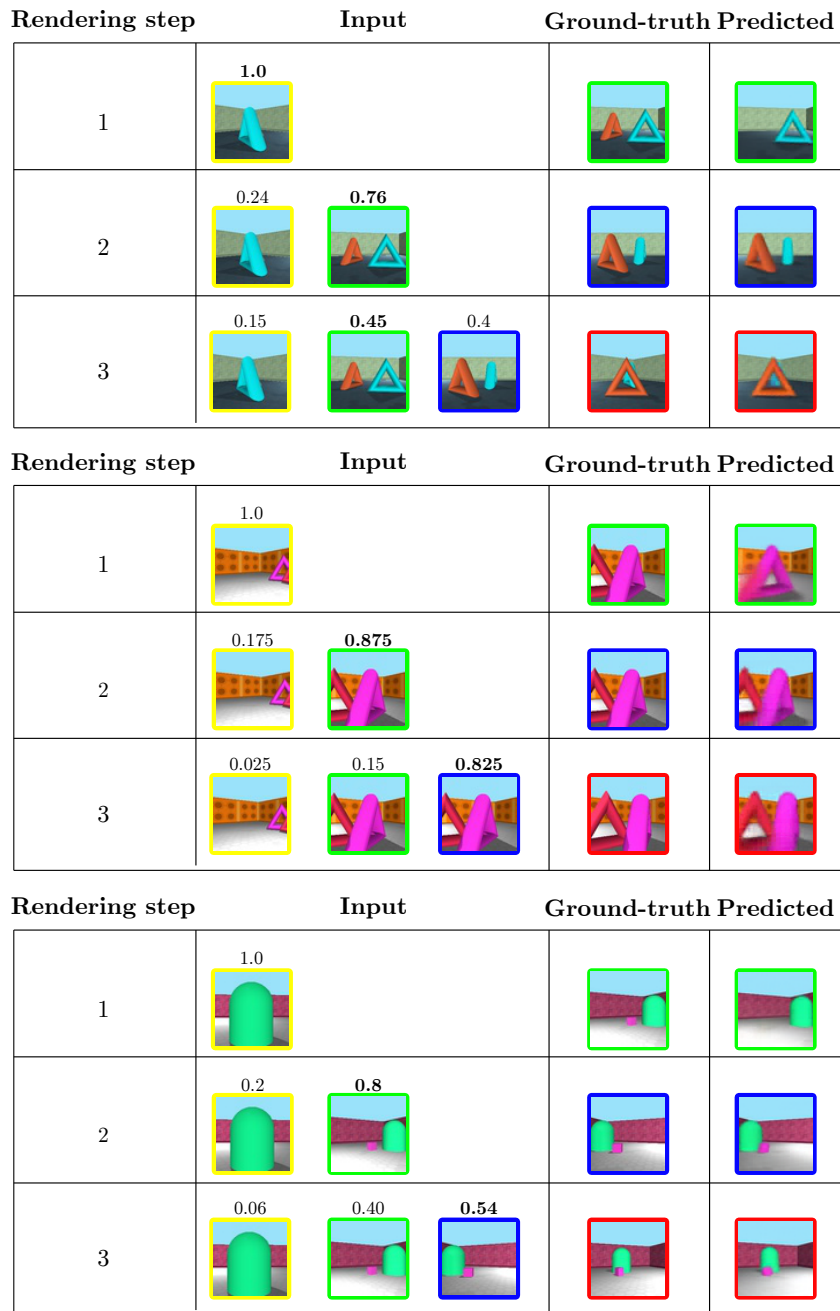


Fig. 12. Visualization of multi-view attention scores at each rendering step produced by our proposed T-GQN model on the Rooms-Ring-Camera (RRC) dataset.

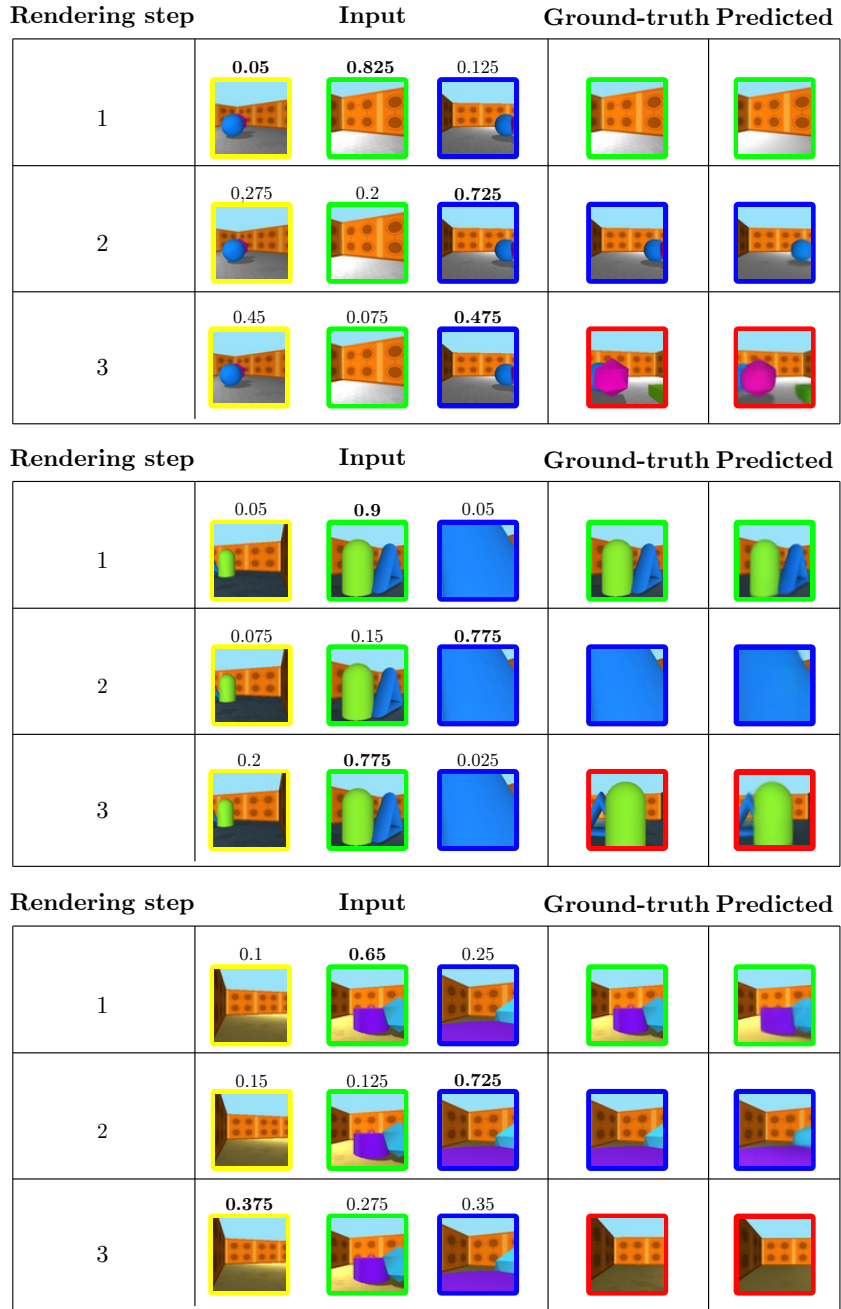


Fig. 13. Visualization of multi-view attention scores at each rendering step produced by our proposed T-GQN model on the Rooms-Free-Camera (RFC) dataset.

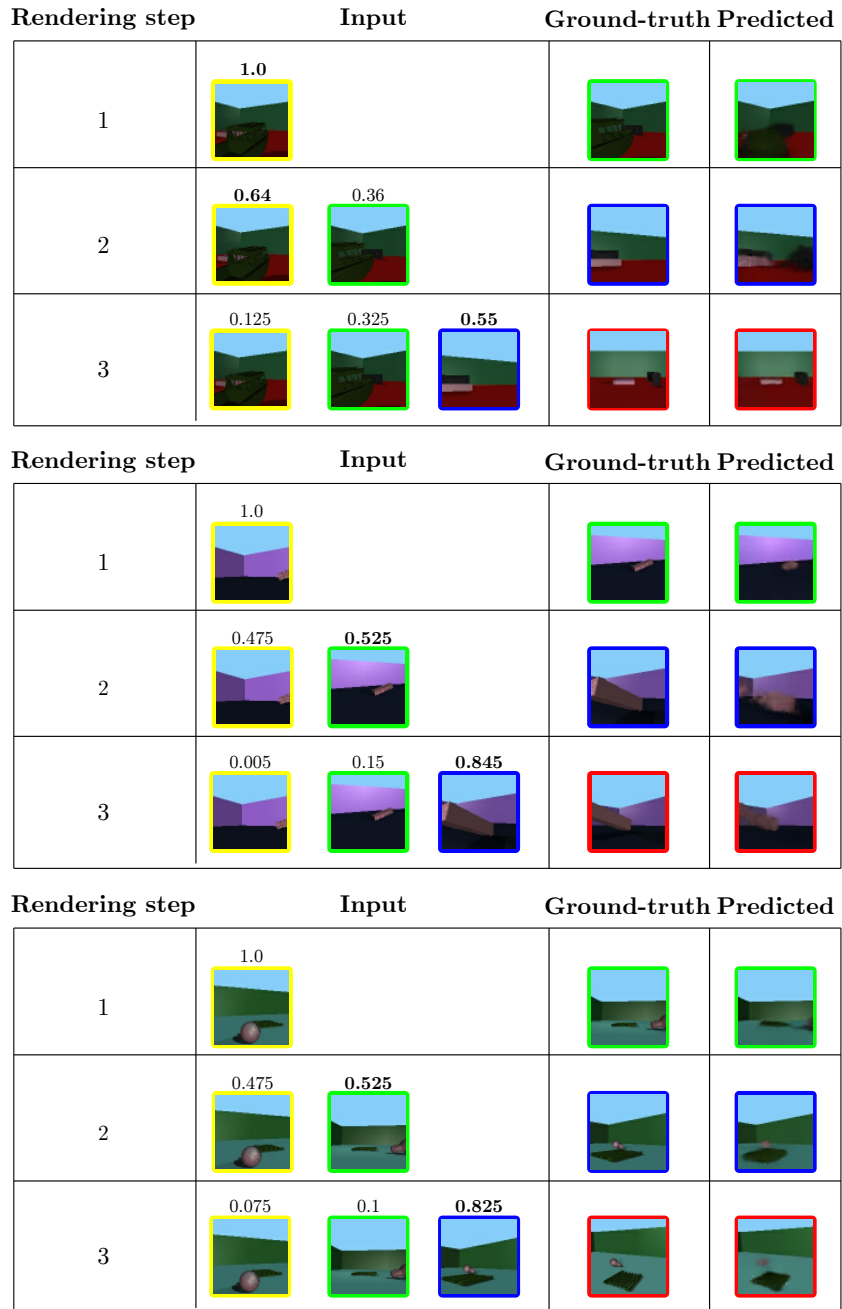


Fig. 14. Visualization of multi-view attention scores at each rendering step produced by our proposed T-GQN model on the Rooms-Random-Objects (RRO) dataset.

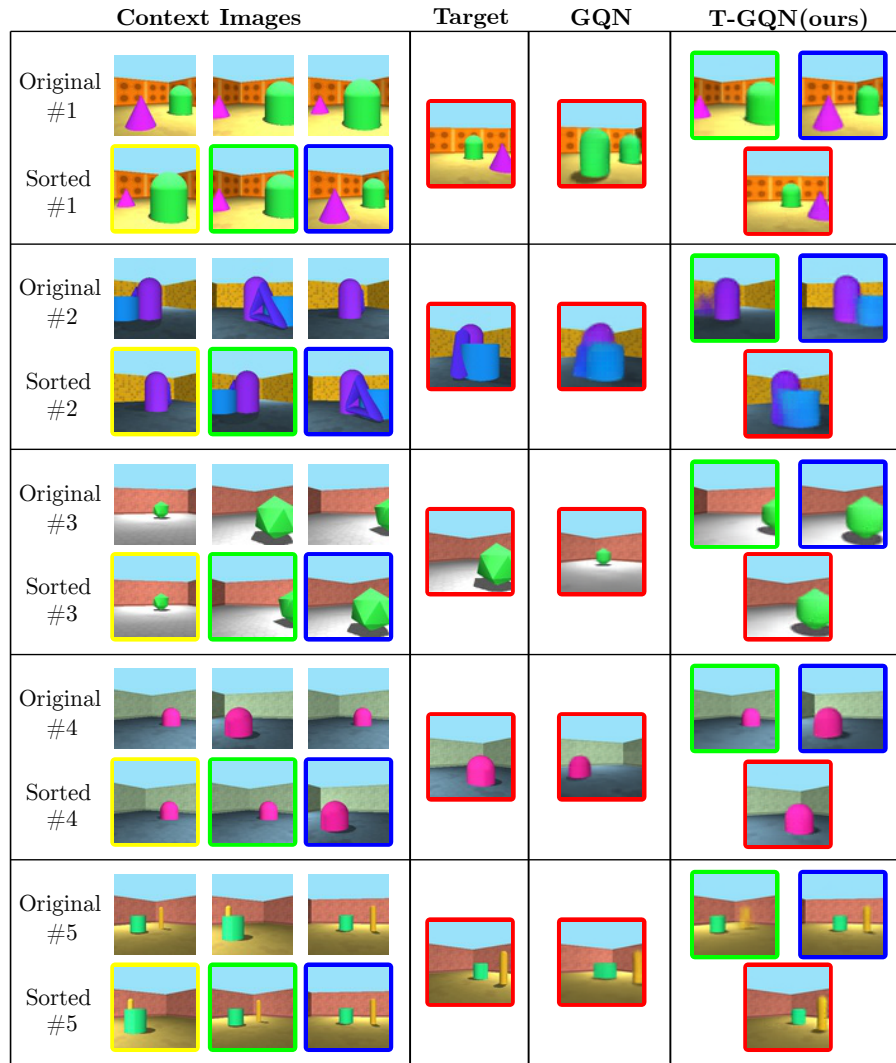


Fig. 15. Example of rendered novel views using our proposed T-GQN (with masking) and GQN on the test set of the Rooms-Ring-Camera (RRC) dataset.

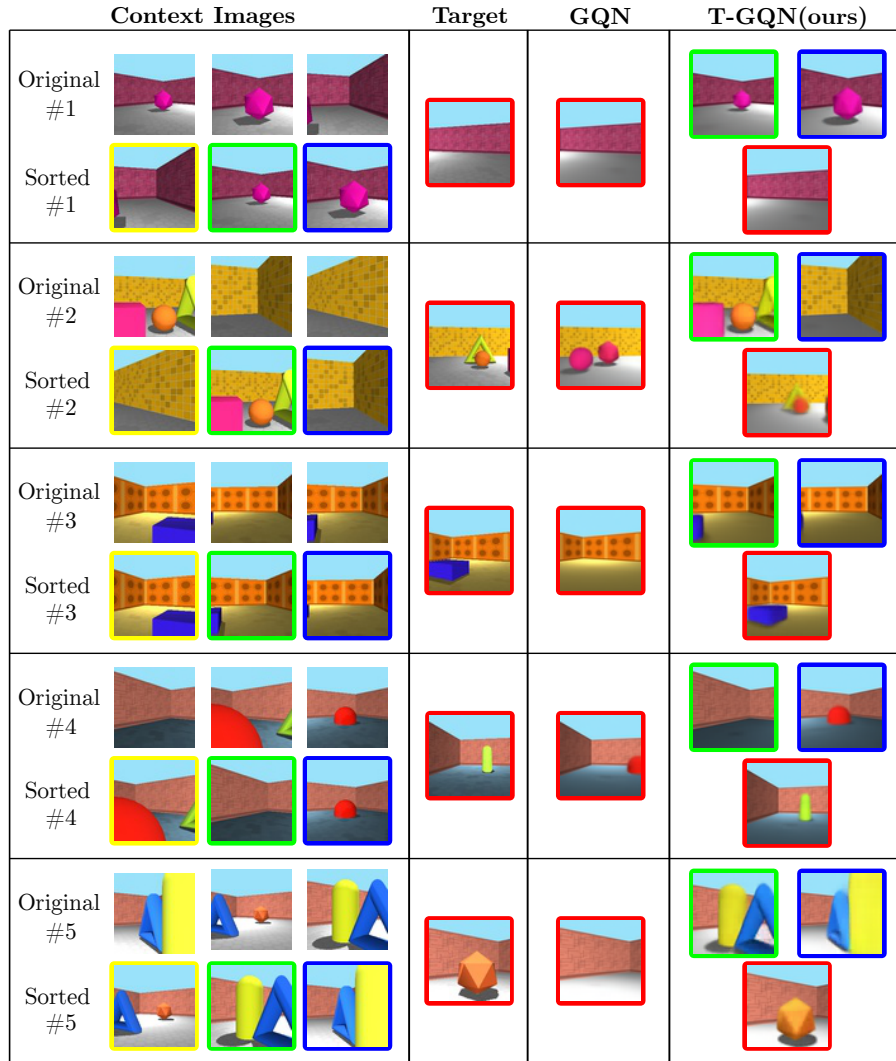


Fig. 16. Example of rendered novel views using our proposed T-GQN (without masking) and GQN on the test set of the Rooms-Free-Camera (RFC) dataset.

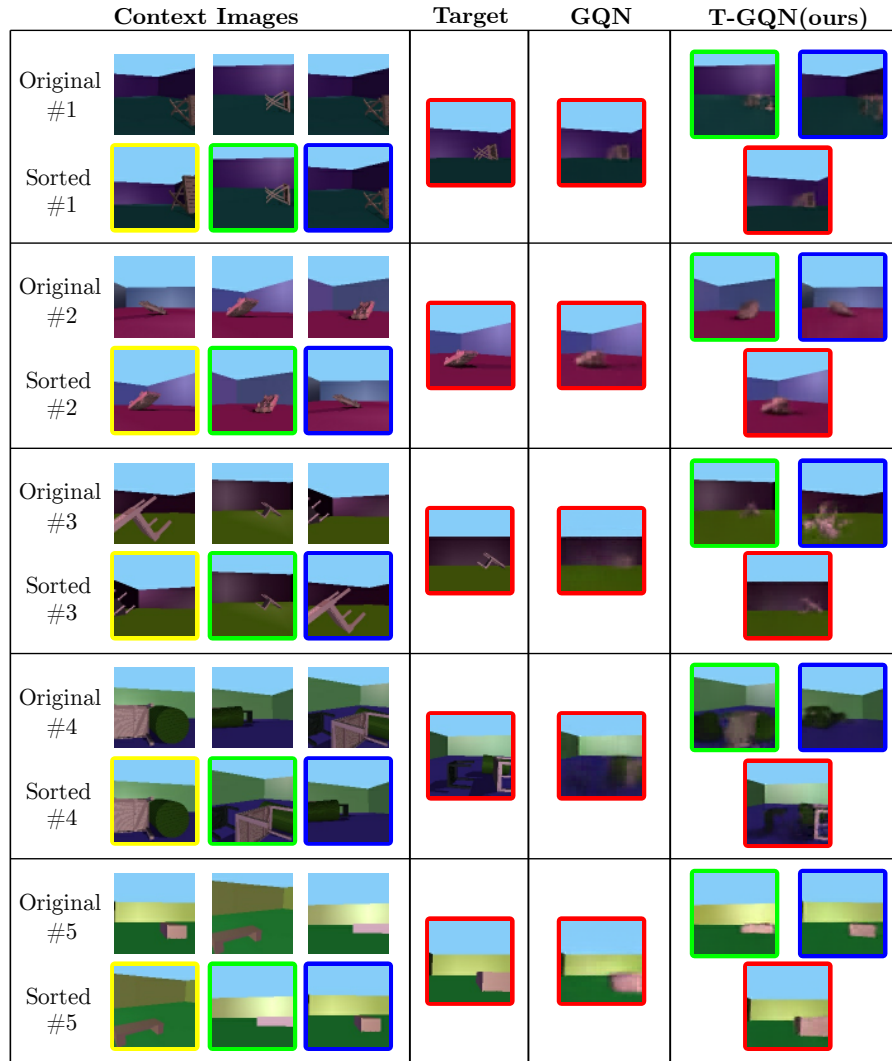


Fig. 17. Example of rendered novel views using our proposed T-GQN (with masking) and GQN on the test set of the Rooms-Random-Objects (RRO) dataset.














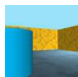
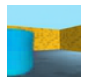
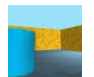
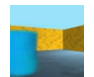









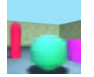



Context image	Target	Predicted			
		T-GQN (using r_1^*)	T-GQN (using r_2^*)	T-GQN (using r_3^*)	T-GQN (full model)
					
					
					
					
					

Fig. 18. Example of rendered novel views using our proposed T-GQN using the sequential rendering decoder (full model) and different multi-view attention scene representations (using r_1^*, r_2^*, r_3^*).